2018 International Conference on Indoor Positioning and Indoor Navigation (IPIN), 24-27 September 2018, Nantes, France

Recursive Bayesian Filters for RSS-based Device-free Localization and Tracking

Ossi Kaltiokallio*‡ ossi.kaltiokallio@aalto.fi
Roland Hostettler† roland.hostettler@aalto.fi
Neal Patwari‡§ npatwari@ece.utah.edu
Riku Jäntti* riku.jantti@aalto.fi

*Department of Communications and Networking, Aalto University, Espoo, Finland
†Department of Electrical Engineering and Automation, Aalto University, Espoo, Finland
‡Department of Electrical and Computer Engineering, University of Utah, Salt Lake City, USA
§Xandem Technology LLC, Salt Lake City, USA

***Abstract*—Received signal strength (RSS)-based device-free localization applications utilize the communication between wireless devices for locating people within the monitored area. The technology is based on the fact that humans cause changes in properties of the wireless channel which is observed in the RSS, enabling localization of people without requiring them to carry any sensor, tag or device. Typically this inverse problem is solved using an empirical model that relates the RSS to location of the sensors and person, and utilizing either an imaging method or a particle filter (PF) for positioning. In this paper, we present an extended Kalman filtering (EKF) solution that incorporates some of the beneficial properties of the PF but has a lower computational overhead. In order to make the EKF work, we also need to reconsider how the measurements are sampled and processed, and a new processing scheme is proposed. The developments are validated using simulations and experimental data, and the results imply: *i)* the non-linear filters outperform a popular imaging method; *ii)* the robustness of the EKF and PF is improved using the proposed processing scheme; and *iii)* the EKF achieves similar performance as the PF as long as the new processing scheme is used.**

***Index Terms*—received signal strength, wireless sensor networks, Bayesian filtering, positioning and tracking**

I. Introduction

Interest towards non-invasive radio frequency (RF) sensing has grown rapidly in the past decade. The technology is built upon the fact that humans alter the propagation characteristics of radio signals and at the receiver, these changes can be quantified using the radio's channel measurements. Research has demonstrated the use of various radio signal measurements for inference including: time delay [1], phase [2], and signal strength [3]; and these have been used for various purposes including: vital sign monitoring [1], activity and gesture recognition [2], and localization [3]. In this paper, we consider narrowband wireless devices that measure the received signal strength (RSS) and we utilize the RSS for localization and tracking purposes.

In RSS-based device-free localization and tracking (DFLT), there are two widely used approaches for locating people: fingerprinting [4], [5], and model-based approaches [3], [6]. Fingerprinting methods use a database of training data labelled with a person's known locations. During runtime, the current set of RSS measurements are compared to those in the database to estimate the current location. Model-based approaches use an a priori model for the changes in RSS with respect to the locations of the sensors and person, and localization is typically performed via imaging [3], [7] or sequential Monte Carlo (SMC) methods [6], [8]. Fingerprinting methods are able to achieve high accuracy also in demanding environments, but the training process is laborious and the performance degrades exponentially as the environment is altered [5]. Model-based approaches can be deployed quickly [9], but the mismatch between the RSS model and measurements results in degraded performance [10].

It is well known in the DFLT community that the model parameters tend to vary between different wireless links and that the dispersion is larger the more cluttered the environment is [11]. A recent work has shown that to overcome this challenge, the model parameters can be estimated during run-time to enable improved localization accuracy in challenging environments [10]. The work uses an imaging method for localization, the estimates are enhanced using fixed-lag smoothing and the model parameters are trained using a batch-processing method. This problem could be addressed more formally using Bayesian estimation where all uncertainties related to target state and model parameters could be taken into account. So far, particle filters (PF) are the only Bayesian filters that have been proposed for DFLT and with these methods, smoothing and parameter estimation are computationally very demanding. This work introduces a non-linear Gaussian filter that is as accurate as the PF but that is computationally much more efficient, especially if smoothing and parameter estimation are considered.

Specifically, we present an extended Kalman filter (EKF) solution for tracking the kinematic state of the target in this paper. In addition, we propose a new processing scheme that enables us to resolve time ambiguities related to sampling and processing and also allows us to solve the state evolution more accurately. The development efforts are demonstrated using simulations and validated with real-world experimental

978-1-5386-5635-8/18/$31.00

data. The results imply that: first, the new processing scheme increases robustness and accuracy of an existing PF solution; second, the new processing scheme makes it possible to use low-complexity non-linear Gaussian filters in DFLT; third, the implemented EKF achieves similar performance as the PF but with reduced computational overhead. The most attractive feature of using low-complexity non-linear Gaussian filters in DFLT is that they enable the use of Gaussian smoothers. These smoothers can be used for approximating marginal likelihoods and parameter posteriors which are needed by various parameter estimation methods such as expectation-maximization algorithms and optimization based methods [12, Ch. 12]. This paper does not address Bayesian parameter estimation but the paper builds a foundation for a system that has such capabilities.

The remainder of the paper is organized as follows. In the next section, related work is discussed. Thereafter, the problem of tracking the kinematic state of the person is formulated and models of the system are introduced. The methodology of the paper is presented in Sections IV and V of which the first concentrates on introducing the tracking algorithms and the latter section concentrates on sampling and processing the RSS measurements. The experiments and results are presented in Section VI and thereafter, conclusions are drawn.

II. Related Work

In RSS-based DFLT, the person is typically located and tracked either using an imaging approach [3], [7], [10] or SMC methods [8], [6], [13]. Radio tomographic imaging (RTI) computes a propagation field image of the monitored area [3], [7], the person is localized from the estimated image, and then a Kalman filter (KF) is used for estimating the kinematic state of the target [14], [10]. The SMC approach is typically solved using a PF where the RSS measurements are directly related to the person's location using either an empirical model [8], [13] or a theoretical propagation model [6], [15]. RTI is computationally efficient, it is robust and it provides a global estimate within the monitored area. As a drawback, information can be lost in the two-step process to first estimate the image and then the location and in addition, discretization of the image inevitably degrades the localization accuracy. The PF solution is more accurate if the RSS-model describes the data well. However, the PF is computationally more demanding, the estimates are local and the filter can diverge. In this paper, we present an EKF solution that is as accurate as the PF but that is computationally less demanding.

The networking requirements of a DFLT systems are well known; the measurements should be gathered within limits of the coherence bandwidth and coherence time of the wireless channel [16]. To meet these limitations, DFLT system are usually designed so that the transmission interval between communications is minimized and typically the systems have a transmission interval from a few milliseconds [10] to tens of milliseconds [13]. The systems use time-division multiple access (TDMA) or similar for exchanging packets [16], [17] and at the end of the communication cycle, the measurements are processed [6], [10]. In the filtering algorithm, it is commonly assumed that the measurements are taken at the same time instant and that the environment does not change within one communication round [6], [10], [13], [8]. This is a clear simplification of the problem that is appropriate if the person remains stationary or if the sampling rate is really high. In this paper, we propose a new processing scheme that resolves the time evolution correctly and we demonstrate that this improves the performance of an existing PF solution and also enables the use of low-complexity non-linear Gaussian filters when tracking a moving target.

III. Problem Formulation

A. Bayesian Filtering

The objective of RSS-based DFLT is to recursively estimate position and velocity of the person using the measurements of L wireless links. This problem can be formulated using a state space model of the form

$$\mathbf{x}_k = \mathbf{f}\left(\mathbf{x}_{k-1}\right) + \mathbf{q}_{k-1}, \tag{1a}$$

$$\mathbf{z}_k = \mathbf{h}\left(\mathbf{x}_k\right) + \mathbf{r}_k, \tag{1b}$$

where $\mathbf{x}_k \in \mathbb{R}^{4\times 1}$ is the person's state and $\mathbf{z}_k \in \mathbb{R}^{L\times 1}$ the mean-removed RSS measurement vector, their noises are assumed Gaussian, that is, $\mathbf{q}_{k-1} \sim \mathcal{N}(\mathbf{0}, \mathbf{Q}_{k-1})$ and $\mathbf{r}_k \sim \mathcal{N}(\mathbf{0}, \mathbf{R}_k)$, $\mathbf{f}(\cdot)$ is the dynamic model of the person, $\mathbf{h}(\cdot)$ is the RSS measurement model and k denotes the time. The mean removed RSS is defined as $\mathbf{z}_k = \tilde{\mathbf{z}}_k - \bar{\mathbf{z}}$, where $\tilde{\mathbf{z}}_k$ is the RSS of the nodes and $\bar{\mathbf{z}}$ is the mean RSS vector computed during an initialization procedure. The DC component contains no information about location of the person and it is typically removed from the RSS in DFLT [10], [8], [13], [6], [7]. We refer to the mean-removed RSS measurements simply as the RSS in the remainder of the paper.

The problem of tracking aims to construct the posterior probability density function (PDF), $p(\mathbf{x}_k|\mathbf{z}_{1:k})$, recursively using the prediction and update stages [12, Ch 4.2]. The prediction step calculates the prior PDF using the Chapman-Kolmogorov equation

$$p(\mathbf{x}_k|\mathbf{z}_{1:k-1}) = \int p(\mathbf{x}_k|\mathbf{x}_{k-1}) p(\mathbf{x}_{k-1}|\mathbf{z}_{1:k-1}) d\mathbf{x}_{k-1}, \tag{2}$$

where it is assumed that $p(\mathbf{x}_{k-1}|\mathbf{z}_{1:k-1})$ is available from the previous time step, $p(\mathbf{x}_k|\mathbf{x}_{k-1})$ is a first order Markov model and the state evolution is assumed known and defined by Eq. (1a). At time k, measurement $\mathbf{z}_k$ becomes available and the prior can be updated using the Bayes' rule

$$p(\mathbf{x}_k|\mathbf{z}_{1:k}) = \frac{p(\mathbf{z}_k|\mathbf{x}_k) p(\mathbf{x}_k|\mathbf{z}_{1:k-1})}{\int p(\mathbf{z}_k|\mathbf{x}_k) p(\mathbf{x}_k|\mathbf{z}_{1:k-1}) d\mathbf{x}_k}, \tag{3}$$

where the likelihood function $p(\mathbf{z}_k|\mathbf{x}_k)$ is defined by Eq. (1b). When $\mathbf{f}(\cdot)$ and $\mathbf{h}(\cdot)$ are linear and the noises Gaussian, Eqs. (2) and (3) can be solved using a KF. However, the optimal KF solution is often intractable because the models are non-linear and/or the noises are non-Gaussian. Thus, sub-optimal methods are often required in Bayesian filtering such as the EKF or PF.

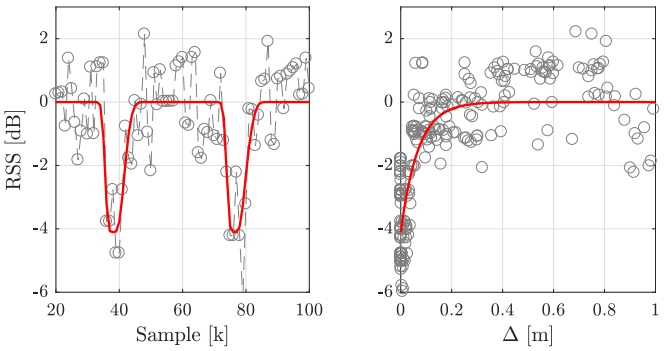

Fig. 1: On the left, z_k (-⊖-) and $h(\mathbf{x}_k)$ (——) as a function of time when a person crosses the link line twice. On the right, z_k and $h(\mathbf{x}_k)$ as a function of Δ.

B. Dynamic Model

In DFLT literature, a common choice for the dynamic model is the second-order kinematic model [13], [14] for which the single dimension dynamics and noise covariance are given by [18, Ch 6.2]

$$\mathcal{F} = \begin{bmatrix} 1 & \tau \\ 0 & 1 \end{bmatrix}, \quad \mathcal{Q} = q \begin{bmatrix} \frac{1}{3}\tau^3 & \frac{1}{2}\tau^2 \\ \frac{1}{2}\tau^2 & \tau \end{bmatrix}, \tag{4}$$

where q is the power spectral density of the process noise and τ is the sampling rate. The state in the two dimensional Cartesian coordinate system is defined as

$$\mathbf{x}_k = \begin{bmatrix} p_x(k) & v_x(k) & p_y(k) & v_y(k) \end{bmatrix}^T$$

where $p_x(k)$ and $p_y(k)$ are coordinates of the person at time k, and the velocity components are denoted as $v_x(k)$ and $v_y(k)$. Using (4), the dynamic model and noise covariance for $\mathbf{x}_k$ are defined as $\mathbf{F} = \text{blkdiag}(\mathcal{F}, \mathcal{F})$, $\mathbf{Q} = \text{blkdiag}(\mathcal{Q}, \mathcal{Q})$ and blkdiag denotes the block-diagonal concatenation of matrices. Now, Eq. (1a) can be written as

$$\mathbf{x}_k = \mathbf{F}\mathbf{x}_{k-1} + \mathbf{q}_{k-1}. \tag{5}$$

C. RSS Measurement Model

Consider link l with transmitter (TX) i and receiver (RX) j that have sensor positions $\mathbf{p}_i$ and $\mathbf{p}_j$ in respective order and generally the coordinates are defined as $\mathbf{p} = \begin{bmatrix} p_x & p_y \end{bmatrix}^T$. The excess path length defines the minimum distance a radio signal travels that is altered by a person located at $\mathbf{p}_k$ at time k and it is given by

$$\Delta_l(k) \triangleq \|\mathbf{p}_i - \mathbf{p}_k\| + \|\mathbf{p}_j - \mathbf{p}_k\| - \|\mathbf{p}_i - \mathbf{p}_j\|, \tag{6}$$

defining an ellipse with TX and RX located at the foci. The person's location can be parametrized using $\Delta_l(k)$ and it has been proposed that it is related to the RSS of link l via [8]

$$h_l(\mathbf{x}_k) \triangleq \phi\, e^{-\Delta_l(k)/\lambda}, \tag{7}$$

where ϕ defines the maximum RSS change when the person is in between the TX-RX pair and λ controls the rate of decay with respect to $\Delta_l(k)$. Considering the measurements of all L links, the complete measurement vector is

$$\mathbf{h}(\mathbf{x}_k) = \begin{bmatrix} h_1(\mathbf{x}_k), & \dots & h_L(\mathbf{x}_k) \end{bmatrix}^T, \tag{8}$$

and the measurement noise covariance is $\mathbf{R}_k = \text{diag}(\begin{bmatrix} \sigma^2_{r,1}, & \sigma^2_{r,2}, & \dots, & \sigma^2_{r,L} \end{bmatrix})$, where diag denotes a square diagonal matrix. In Fig. 1, z_k and $h(\mathbf{x}_k)$ shown for a single link as a person crosses the *link-line* twice, that is, the straight imaginary line connecting the TX-RX pair.

IV. Tracking Algorithms

Given models of the system and assuming the noises Gaussian, it is straightforward to implement a tracking algorithm for the RSS-based DFLT problem. In the following, we first present the extended Kalman filter solution. Then, the commonly used particle filter approach is presented [8], [13], [6] and thereafter, a Kalman filter solution used for example in [10], [14] is given. All three solutions are presented so that the reader can easily understand on which parts the filtering algorithms differ and on which part they are the same.

A. Extended Kalman Filter

Given that $\mathbf{F}$ is linear and $\mathbf{h}(\cdot)$ non-linear, the prediction (9a)-(9b) and update (9c)-(9f) steps of the first order additive noise EKF are [12, Ch 5.2]

$$\mathbf{x}_k^- = \mathbf{F}\mathbf{x}_{k-1}, \tag{9a}$$
$$\mathbf{P}_k^- = \mathbf{F}\mathbf{P}_{k-1}\mathbf{F}^T + \mathbf{Q}_{k-1}, \tag{9b}$$
$$\mathbf{S}_k = \mathbf{H}_\mathbf{x}(\mathbf{x}_k^-)\mathbf{P}_k^-\mathbf{H}_\mathbf{x}^T(\mathbf{x}_k^-) + \mathbf{R}_k, \tag{9c}$$
$$\mathbf{K}_k = \mathbf{P}_k^-\mathbf{H}_\mathbf{x}^T(\mathbf{x}_k^-)\mathbf{S}_k^{-1}, \tag{9d}$$
$$\mathbf{x}_k = \mathbf{x}_k^- + \mathbf{K}_k\left(\mathbf{z}_k - \mathbf{h}(\mathbf{x}_k^-)\right), \tag{9e}$$
$$\mathbf{P}_k = \mathbf{P}_k^- - \mathbf{K}_k\mathbf{S}_k\mathbf{K}_k^T. \tag{9f}$$

The elements for the Jacobian of $h_l(\mathbf{x}_k)$ given in (7) are defined as

$$\begin{bmatrix} \frac{\delta h_l}{\delta p_x} & \frac{\delta h_l}{\delta p_y} \end{bmatrix}^T = \frac{h_l(\mathbf{x}_k)}{\lambda}\left(\frac{\mathbf{p}_{T_l} - \mathbf{p}_k}{\|\mathbf{p}_{T_l} - \mathbf{p}_k\|} + \frac{\mathbf{p}_{R_l} - \mathbf{p}_k}{\|\mathbf{p}_{R_l} - \mathbf{p}_k\|}\right),$$

the Jacobian for link l is

$$\mathcal{H}_l(\mathbf{x}_k) = \begin{bmatrix} \frac{\delta h_l}{\delta p_x} & 0 & \frac{\delta h_l}{\delta p_y} & 0 \end{bmatrix}, \tag{10}$$

and the complete Jacobian for the L links is

$$\mathbf{H}_\mathbf{x}(\mathbf{x}_k) = \begin{bmatrix} (\mathcal{H}_1(\mathbf{x}_k))^T, \dots, (\mathcal{H}_L(\mathbf{x}_k))^T \end{bmatrix}^T. \tag{11}$$

It is to be noted that the measurements of the L links can be sampled at different time instances and the filter recursion can be performed link at a time since the measurements are assumed independent. The recursion is performed as follows: i) propagate $\mathbf{x}_k^-$ and $\mathbf{P}_k^-$ at time k ii) update the elements of $\mathbf{H}_\mathbf{x}(\mathbf{x}_k^-)$ and $\mathbf{h}(\mathbf{x}_k^-)$ corresponding to the links sampled at time k before the update stage; iii) only the lth row of $\mathbf{H}_\mathbf{x}(\mathbf{x}_k^-)$, $\mathbf{z}_k$, $\mathbf{h}(\mathbf{x}_k^-)$ and lth diagonal element of $\mathbf{R}_k$ are used when updating link l; and iv) $\mathbf{x}_k^-$ and $\mathbf{P}_k^-$ are updated using (9e) and (9f) after each iteration.

TABLE I: Measurements, models and filtering equations

	PF	EKF	KF
Measurement	$\mathbf{z}_k$ (1b)		$\mathbf{y}_k$ (19)
Dynamic model	$\mathbf{F}$ and $\mathbf{Q}$ in (5)		
Meas. model	$\mathbf{h}(\mathbf{x}_k)$ and $\mathbf{R}$ (8)		$\mathbf{H}$ and $\mathbf{N}$ (20)
Prediction Step	(14a)	(9a)-(9b)	
Update Step	(14b)	(9c)-(9f)	(21a)-(21d)

B. Particle Filter

The PF approximates the posterior PDF using a set of weighted particles [12, Ch 7]

$$p(\mathbf{x}_k|\mathbf{z}_{1:k}) \approx \sum_{i=1}^{M} w_k^i \delta\left(\mathbf{x}_k - \mathbf{x}_k^i\right), \tag{12}$$

where w_k^i and $\mathbf{x}_k^i$ are the weight and state of particle i, $\delta(\cdot)$ is the Dirac delta function, M is the number of particles and $\sum_{i=1}^{M} w_k^i = 1$. The weights in (12) are defined as

$$w_k^i \propto w_{k-1}^i \frac{p(\mathbf{z}_k|\mathbf{x}_k^i)p(\mathbf{x}_k^i|\mathbf{x}_{k-1}^i)}{q(\mathbf{x}_k^i|\mathbf{x}_{0:k-1}^i, \mathbf{z}_{1:k})}, \tag{13}$$

where $q(\mathbf{x}_k^i|\mathbf{x}_{0:k-1}^i, \mathbf{z}_{1:k})$ is the importance density. The sequential importance resampling (SIR) filter is commonly used in DFLT literature and the algorithm can be implemented by choosing the prior density $p(\mathbf{x}_k^i|\mathbf{x}_{k-1}^i)$ as importance density $q(\mathbf{x}_k^i|\mathbf{x}_{0:k-1}^i, \mathbf{z}_{1:k})$, and applying the resampling step at every time index [19]. Because resampling is applied at every time step, $w_k^i = \frac{1}{M}\ \forall i$ simplifying (13) to $w_k^i \propto p(\mathbf{z}_k|\mathbf{x}_k^i)$. Thus, the prediction and update stages of the SIR filter can be performed for each particle i as

$$\mathbf{x}_k^i \sim p\left(\mathbf{x}_k|\mathbf{x}_{k-1}^i\right), \tag{14a}$$

$$w_k^i = \prod_{l=1}^{L} \exp\left(-\frac{(z_l(k) - h_l(\mathbf{x}_k^i))^2}{2\sigma_r^2}\right), \tag{14b}$$

where $z_l(k)$ is the RSS measurement for link l at time k and $h_l(\cdot)$ is given in (7). After (14a) and (14b) are calculated for each particle at time step k, the weights are normalized to sum to unity using $w_k^i = w_k^i / \sum_{i=1}^{M} w_k^i$, resampling is performed thereafter and the approximate posterior PDF is given by (12). The readers are referred to [12] and [19] for more details on PFs.

C. Kalman Filtering Solution

The problem at hand can be formulated so that the measurement model is also linear using radio tomographic imaging. In RTI, a discretized propagation field image of the monitored area is computed and then the person is located from the estimated image. Thereafter, a KF can be used to estimate the kinematic state of the target. In the following, we first present RTI and thereafter, the KF algorithm is summarized.

In RTI, the RSS of the L links are modeled using [3]

$$\mathbf{z}_k = \mathbf{A}\mathbf{b}_k + \mathbf{r}_k, \tag{15}$$

where $\mathbf{A} \in \mathbb{R}^{L\times N}$ is a weight matrix that relates the spatial loss field $\mathbf{b}_k \in \mathbb{R}^{N\times 1}$ to the RSS $\mathbf{z}_k \in \mathbb{R}^{L\times 1}$, $\mathbf{r}_k$ is the measurement noise defined in (1b) and N is the pixel number. The minimum mean square error estimate (MMSE) for the model in (15), with Gaussian prior and noise is

$$\hat{\mathbf{b}}_k = \left(\mathbf{A}^T\mathbf{R}^{-1}\mathbf{A} + \mathbf{B}^{-1}\right)^{-1}\mathbf{A}^T\mathbf{R}^{-1}\mathbf{z}_k \tag{16}$$

where $\mathbf{B}$ is the covariance matrix of the image. The element of $\mathbf{A}$ for link l and pixel n is [10]

$$\{\mathbf{A}\}_{l,n} = \frac{1}{\sqrt{d_l}} \exp\left(-\Delta_{l,n}/\lambda\right), \tag{17}$$

where $d_l = \|\mathbf{p}_{T_l} - \mathbf{p}_{R_l}\|$ is the link length, $\Delta_{l,n}$ the excess path length and λ controls size of the weighting ellipse. Note the similarity of Eqs. (17) and (7). The covariance matrix $\mathbf{R}$ is diagonal with elements σ_r^2 and $\mathbf{B}$ for pixels m and n is defined as [3]

$$\{\mathbf{B}\}_{m,n} = \sigma_b^2 \exp\left(-d_{m,n}/d_s\right), \tag{18}$$

where σ_b^2 is the pixel variance, $d_{m,n} = \|\mathbf{p}_m - \mathbf{p}_n\|$ distance between the pixels and d_s is a user defined space constant. From the estimated image $\hat{\mathbf{b}}_k \in \mathbb{R}^{N\times 1}$, the person can be localized by finding pixel n with highest intensity

$$\mathbf{y}_k = \begin{bmatrix} p_x(n) & p_y(n) \end{bmatrix}^T, \text{where} \quad n = \arg\max \hat{\mathbf{b}}_k, \tag{19}$$

and p_x and p_y denote the pixel coordinates. Now, (1b) can be re-written for RTI as

$$\mathbf{y}_k = \mathbf{H}\mathbf{x}_k + \mathbf{n}_k, \text{ where } \quad \mathbf{H} = \begin{bmatrix} 1 & 0 & 0 & 0 \\ 0 & 0 & 1 & 0 \end{bmatrix} \tag{20}$$

and the measurement noise covariance is $\mathbf{N}_k = \sigma_n^2\mathbf{I}_2$.

The RTI + KF approach and non-linear filters use the same dynamical model whereas the measurement models are different; the non-linear filters directly relate the RSS to the person's location whereas the RTI + KF approach first uses RTI to locate the target and thereafter, the KF is used to track the kinematic state. Thus, the prediction step of the KF can be done using Eqs. (9a)-(9b) and the update step is given by [12, Ch 4.3]

$$\mathbf{S}_k = \mathbf{H}\mathbf{P}_k^-\mathbf{H}^T + \mathbf{N}_k, \tag{21a}$$

$$\mathbf{K}_k = \mathbf{P}_k^-\mathbf{H}^T\mathbf{S}_k^{-1}, \tag{21b}$$

$$\mathbf{x}_k = \mathbf{x}_k^- + \mathbf{K}_k\left(\mathbf{y}_k - \mathbf{H}\mathbf{x}_k^-\right), \tag{21c}$$

$$\mathbf{P}_k = \mathbf{P}_k^- - \mathbf{K}_k\mathbf{S}_k\mathbf{K}_k^T. \tag{21d}$$

The models and filtering equations are summarized in Table I for the three approaches. Note that measurement noise covariance are different for the filters, $\mathbf{R}_k$ is related to the RSS for the non-linear filters, whereas for the RTI + KF solution $\mathbf{N}_k$ is related to the error of locating the target from the image. In the subsequent sections, the RTI + KF solution is referred shortly as KF.

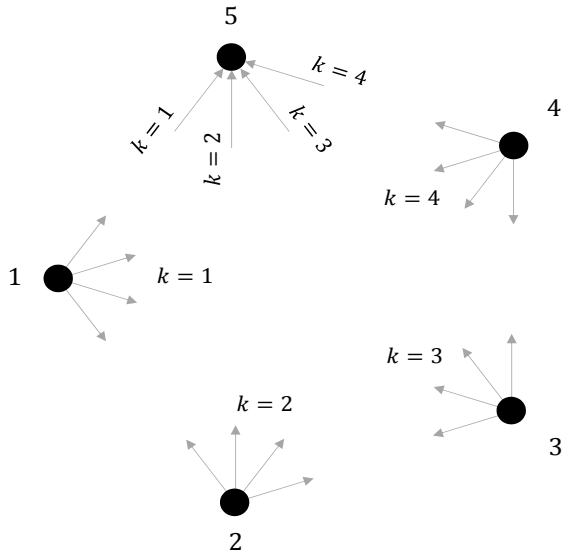

Fig. 2: An example of the token passing protocol

V. Sampling and Processing

In RSS-based DFLT, the transceivers are programmed to transmit and receive packets from other sensors of the network. Typically, the communication schedule follows a token passing protocol where one sensor transmits at a time while the others are in reception mode. After transmission, the turn is assigned to the next node in the schedule following the sensor IDs in sequential order. In the packets, the nodes include the most recent RSS associated with the transmissions of others'. An example of the token passing protocol is illustrated in Fig. 2 using a network of five nodes and as an example, the payload of the transmission of node 5 at $k = 5$ is

$$\mathbf{z}_5(5) = \begin{bmatrix} z_{5,1}(1) & z_{5,2}(2) & z_{5,3}(3) & z_{5,4}(4) & 0 \end{bmatrix},$$

where $z_{i,j}(k)$ denotes RSS of the packet that is transmitted by node j and received by node i at time k.

Let the wireless network consist of S nodes, then, when the last node in the schedule transmits at time k the payload of the packet is

$$\mathbf{z}_S(k) = \begin{bmatrix} z_{S,1(k-S+1)} & z_{S,2(k-S+2)} & \cdots & z_{S,S-1(k-1)} & 0 \end{bmatrix}.$$

Typically a base station listens to the ongoing transmissions and it stacks the packets to form a measurement matrix

$$\mathbf{Z}(k) = \begin{bmatrix} \mathbf{z}_1{}_{(k-S+1)}{}^T & \cdots & \mathbf{z}_S{}_{(k)}{}^T \end{bmatrix}^T \tag{23}$$

before processing. The elements of $\mathbf{Z}$ are defined at time k as

$$\mathbf{Z}(k) = \begin{bmatrix} 0 & z_{1,2(k-2S+2)} & \cdots & z_{1,S(k-S)} \\ z_{2,1(k-S+1)} & 0 & \cdots & z_{2,S(k-S)} \\ \vdots & \vdots & \ddots & \vdots \\ z_{S,1(k-S+1)} & z_{S,2(k-S+2)} & \cdots & 0 \end{bmatrix}.$$

In the following, we first present how time evolution is considered in related works and thereafter, we propose an alternative formulation that accounts for the time evolution precisely.

A. Batch Processing

Ideally, all nodes could transmit and receive simultaneously so that the elements of $\mathbf{Z}(k)$ would be sampled at the same time index and the propagation channel could be considered stationary within one communication cycle. This is not realistic with simplistic narrowband radios that do not have MIMO capabilities and typically $\mathbf{Z}(k)$ is given as expressed in (23). We refer to this scenario as *batch processing* and in the tracking algorithms, $\mathbf{Z}(k)$ is converted to a $L = S^2 \times 1$ dimensional column vector and denoted as $\mathbf{z}(k)$. In batch processing, the elements of $\mathbf{z}(k)$ are assumed to be sampled at the same time instant so that the sampling rate is $\tau = S \cdot \tau_{tx}$, where τ_{tx} is transmission interval of the nodes. This is a clear simplification of the problem but which is commonly made in related works [8], [13], [6]. This simplification is justified if the sampling rate is very high or if the person is stationary.

B. Sequential Processing

The dynamics of the person can be taken into account more accurately, if the measurements are processed according to their true time of transmission. In this case, the sampling rate is $\tau = \tau_{tx}$ and the measurement vector is defined as $\mathbf{z}_i' \triangleq \text{row}_i\{\mathbf{Z}\}$. The downside of using $\mathbf{z}_i'$ is that the RSS measurements are taken at different time samples and that the vector is an average description of the propagation channel within that communication round. The better alternative is to use $\mathbf{z}_i \triangleq \text{col}_i\{\mathbf{Z}\}$, that is, the ith column of $\mathbf{Z}$. The elements of $\mathbf{z}_i$ are associated to the same time instant as long as the measurements are delayed so that at time k, the measurements of time $k-S+1$ are used. As an example, when the last node in the schedule transmits at time k, $\mathbf{z}_1(k-S+1)$ becomes available at the base station. We refer to this sampling scenario as *sequential processing* and $\mathbf{z}(k)$ is now an $L = S \times 1$ dimensional column vector. As an example, $\mathbf{z}(k)$ for the first node is defined as

$$\mathbf{z}(k) = \begin{bmatrix} 0 & z_{2,1(k-S+1)} & \cdots & z_{S,1(k-S+1)} \end{bmatrix}^T,$$

VI. Experimental Validation

In this section, performance of the filters are evaluated using the different processing procedures described in Section V. Followed by the experimental setup description, the filters are numerically evaluated and the effect of sampling rate is analyzed. Thereafter, performance of the filters is investigated using experimental data gathered in an open indoor environment. In the experimental results section, the RSS is modeled using (7) and it is assumed that the parameters for each link are known. The parameters are derived using the known location of the person and the training algorithm described in [10]. In the following sections, we do not present experimental results for an RTI method that processes the measurements sequentially since this would require an alternative approach for estimating the images then the one given in (16).

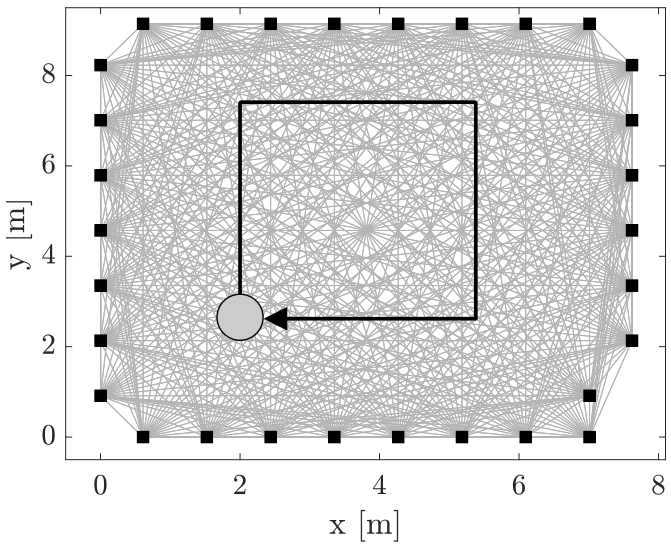

Fig. 3: The experimental setup. In the figure, the wireless nodes are illustrated with ■ and the links using —. The target is presented with ● and trajectory with ——.

A. Experimental Setup

The used wireless sensors are Texas Instruments CC2531 USB dongles operating at the 2.4 GHz ISM band and the sensors communicate in TDMA fashion as explained in [17]. The experiments are conducted using 30 sensors that are deployed as illustrated in Fig. 3 to cover an area of 70m^2. The target moves along the trajectory shown in the figure with a constant speed of 1 m/s. In the numerical results section, measurements $z_l(\cdot)$ are generated with (7) using $\phi = -5$, $\lambda = 0.03$ and corrupted by i.i.d. Gaussian noise with variance $\sigma_r^2 = 1$. The power spectral density of the process noise is set to $q = 1$. The parameters of RTI + KF are: $\sigma_b^2 = 0.002$, $d_s = 2$, $\sigma_n^2 = 0.5$ and the pixel size is set to $d_p = 0.2$ m. The filters are initialized using known position and velocity of the person and diagonal elements of $\mathbf{P}$ are set to 0.1. The PF uses $M = 1000$ particles.

With each sampling rate, sampling scenario and filter combination, 100 Monte Carlo simulations are performed. The filters are evaluated using the root-mean-square error (RMSE) of position $\bar{e}_p$ and velocity $\bar{e}_v$ estimates. As an example, the RMSE for position is defined as

$$\bar{e}_p = \sqrt{\frac{1}{K}\sum_{k=1}^{K}(e_p(k))^2},$$

where the distance error at sample k is calculated as $e_p(k) = \sqrt{(p_x(k) - \hat{p}_x(k))^2 + (p_y(k) - \hat{p}_y(k))^2}$, in which p_x and p_y denote the true coordinates and the hat accent indicates the estimate. In addition, we use the ratio of measurement within a defined threshold for examining robustness of the filters. The metric is defined as

$$\rho_{\%} = K_{in}/K \cdot 100\%,$$

TABLE II: Performance of the filters ($\tau = 0.1$ s)

	$\bar{e}_p$ [m]	$\bar{e}_v$ [m/s]	$\rho_{\%}$ [m]
Batch KF	0.133	0.434	100.0
Batch EKF	0.052	0.310	100.0
Batch PF	0.047	0.331	100.0
Recursive EKF	0.032	0.303	100.0
Recursive PF	0.033	0.308	100.0

where K is the total number of estimates and K_{in} is the number of estimates within one meter of the true location. Typically, the filter has diverged to the incorrect trajectory if the estimate is a meter or further from the true position.

B. Numerical Results

In Fig. 4, the evaluation metrics are illustrated as a function of communication cycle length, and in Table II, the results are summarized for $\tau = 0.1$ s. As shown in the figure, the EKF and PF yield comparative accuracy when the filters do not diverge ($\rho_{\%} = 100\%$) whereas the KF has notably higher RMS errors due to the limited resolution of the discretized images. On the other hand, the KF is most robust of the three filters and it never diverges since the images provide a global estimate.

There are two clear advantages of processing the measurements sequentially. First, the measurement ambiguity is resolved, that is, z_k and $h(\mathbf{x}_k)$ represent the same time instance. This is not true with the batch estimator since z_k are taken over the entire communication cycle and it is assumed that $h(\mathbf{x}_k)$ is taken at a single time instant within that communication cycle. The second advantage is that the dynamics of the person can be taken into account more accurately since the sampling rate is higher and the estimates can be updated more frequently. In more rigorous terms, the posterior PDF estimates of the EKF and PF approximate the true state more accurately when time ambiguity is resolved, and the prior PDF of the non-linear filters is more accurate when the time interval of the prediction step is small.

The proposed processing scheme makes the EKF implementation more robust as shown in Fig. 4. As an example, the EKF encounters divergency issues already when $\tau > 0.3$ s using batch processing whereas $\tau > 1$ s when sequential processing is used. Such an enhancement is mandatory to make the EKF work in real world applications as we will demonstrate in the next section. It is to be noted that the PF solution is much more robust to modeling errors since it does not approximate the filtering distribution using a Gaussian approximation but instead, it uses a set of weighted particles. The particle approximation is superior to the Gaussian approximation if the posterior PDF is multimodal, severe non-linearities exist and unexpected modeling errors are encountered.

C. Experimental Results

Results of the experiment are summarized in Table III and as shown, the EKF is unable to track the person in this experiment when batch processing is used. Divergence of the

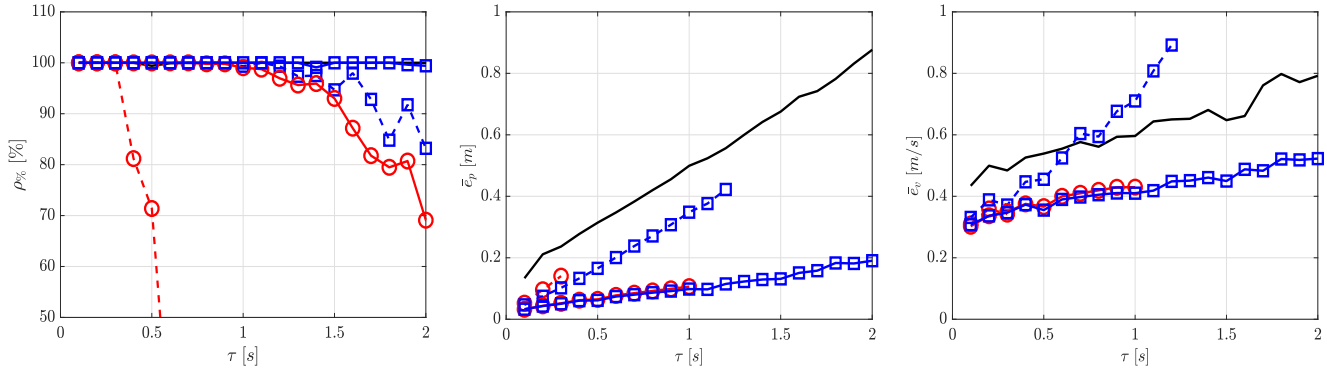

(a) (b) (c)

Fig. 4: In (a), $\rho_{\%}$ as a function of τ illustrating robustness of the filters. In (b) and (c), RMS position and velocity errors in corresponding order. In the figures, the different filters are illustrated using: batch KF (——); batch EKF (-⊖-); sequential EKF (—⊖—); batch PF (-⊟-); sequential PF (—⊟—).

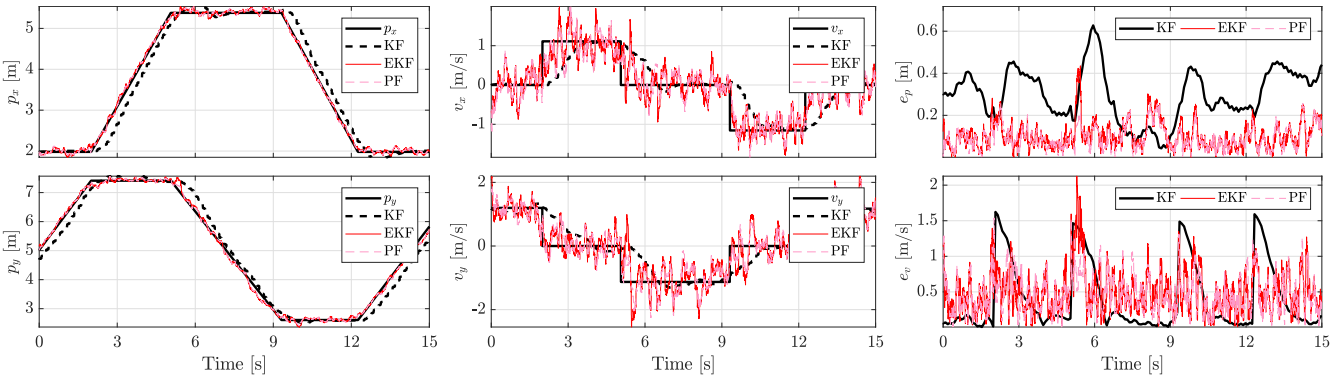

(a) (b) (c)

Fig. 5: Estimation accuracy with the three filters. The coordinate estimates in (a); the velocity estimates in (b); and the positioning and velocity errors in (c).

TABLE III: Performance of the filters

	$\bar{e}_p$ [m]	$\bar{e}_v$ [m/s]
Batch KF	0.354	0.635
Batch EKF	–	–
Batch PF	0.145	0.595
Recursive EKF	0.129	0.569
Recursive PF	0.122	0.538

filter is mainly caused by batch processing and the reasons elaborated above, but also modeling errors have a significant impact. The PF is much more robust to such errors and the filter is able to track the target successfully in this experiment outperforming the KF solution. When sequential sampling is used, the positioning accuracy of the PF solution improves slightly. More importantly, the EKF is also able to track the target and performance of the filters is demonstrated in Fig. 5. As shown, the non-linear filters are able to the track the person with high accuracy, the EKF and PF yield very similar performance and in the figures, the lines of the filters overlap one another in most parts. In the figure, the lag caused by batch processing and computing the images over the entire communication cycle is clearly visible in the KF solution. The non-linear filters are advantageous in this regard since they can directly relate the measurements to the person's kinematic state and timing ambiguities can be resolved.

The average computation times of the filters per communication cycle are KF: 1.1 ms, EKF: 10.9 ms and PF: 30.2 ms using a Matlab implementation and a standard laptop equipped with a 2.70 GHz Intel Core i7-4800MQ processor and 16 GB of RAM. All filters can easily be implemented in real-time since in the experiment, one communication cycle takes 87 ms on average. However, if computational resources are limited one may prefer an EKF over a PF. On the other hand, if our aim was to estimate the model parameters of the links simultaneously or Bayesian smoothing was used to enhance

the state estimates with a given latency, the EKF solution would be more tractable because in these problems the PF is computationally very demanding. For example, the SIR particle smoother requires resampling the state histories but also keeping the full sample histories [12, Ch. 11].

VII. Conclusions

In this paper, a new processing scheme for RSS-based DFLT is presented which enables us to resolve time ambiguities related to processing of the measurements. In addition, it allows us to take the time evolution into account more accurately. It is shown that the new processing scheme increases robustness of a PF solution, the de facto Bayesian filter used for tracking in RSS-based DFLT. In addition, the processing scheme makes it possible to use low-complexity non-linear Gaussian filters in DFLT and in the paper, we present an EKF solution. The simulations and experimental results imply that the EKF achieves comparative performance as the PF in terms of tracking accuracy but the computational overhead of the EKF is significantly lower. The EKF solution enables new and interesting research directions related to Bayesian smoothing and parameter estimation, and these topics will be explored in our future research.

Acknowledgments

This work is based upon work funded by Academy of Finland Project #299099 and #295080. This material is also based upon work supported in part by the U.S. ARO under grant #69215CS.

References

[1] F. Adib, H. Mao, Z. Kabelac, D. Katabi, and R. C. Miller, "Smart homes that monitor breathing and heart rate," in *Proceedings of the 33rd Annual ACM Conference on Human Factors in Computing Systems*, 2015, pp. 837–846.

[2] Q. Pu, S. Gupta, S. Gollakota, and S. Patel, "Whole-home gesture recognition using wireless signals," in *Proceedings of the 19th Annual International Conference on Mobile Computing and Networking*, 2013, pp. 27–38.

[3] N. Patwari and P. Agrawal, "Effects of correlated shadowing: Connectivity, localization, and RF tomography," in *Information Processing in Sensor Networks, 2008 International Conference on*, 2008, pp. 82–93.

[8] Y. Li, X. Chen, M. Coates, and B. Yang, "Sequential Monte Carlo radio-frequency tomographic tracking," in *Acoustics, Speech and Signal Processing, 2011 IEEE International Conference on*, 2011, pp. 3976–3979.

[4] C. Xu, B. Firner, R. S. Moore, Y. Zhang, W. Trappe, R. Howard, F. Zhang, and N. An, "SCPL: Indoor device-free multi-subject counting and localization using radio signal strength," in *Information Processing in Sensor Networks, 2013 ACM/IEEE International Conference on*, 2013, pp. 79–90.

[5] B. Mager, P. Lundrigan, and N. Patwari, "Fingerprint-based device-free localization performance in changing environments," *IEEE Journal on Selected Areas in Communications*, vol. 33, no. 11, pp. 2429–2438, Nov 2015.

[6] Z. Wang, H. Liu, S. Xu, X. Bu, and J. An, "A diffraction measurement model and particle filter tracking method for RSS-based DFL," *IEEE Journal on Selected Areas in Communications*, vol. 33, no. 11, pp. 2391–2403, Nov 2015.

[7] J. Wilson and N. Patwari, "Radio tomographic imaging with wireless networks," *IEEE Transactions on Mobile Computing*, vol. 9, no. 5, pp. 621–632, May 2010.

[9] D. Maas, J. Wilson, and N. Patwari, "Toward a rapidly deployable radio tomographic imaging system for tactical operations," in *38th Annual IEEE Conference on Local Computer Networks - Workshops*, 2013, pp. 203–210.

[10] O. Kaltiokallio, R. Jäntti, and N. Patwari, "ARTI: an adaptive radio tomographic imaging system," *IEEE Transactions on Vehicular Technology*, vol. 66, no. 8, pp. 7302–7316, Aug 2017.

[11] O. Kaltiokallio, M. Bocca, and N. Patwari, "A fade level-based spatial model for radio tomographic imaging," *IEEE Transactions on Mobile Computing*, vol. 13, no. 6, pp. 1159–1172, June 2014.

[12] S. Särkkä, *Bayesian Filtering and Smoothing*. Cambridge University Press, 2013.

[13] Y. Guo, K. Huang, N. Jiang, X. Guo, Y. Li, and G. Wang, "An exponential-Rayleigh model for RSS-based device-free localization and tracking," *IEEE Transactions on Mobile Computing*, vol. 14, no. 3, pp. 484–494, March 2015.

[14] J. Wilson and N. Patwari, "See-through walls: Motion tracking using variance-based radio tomography networks," *IEEE Transactions on Mobile Computing*, vol. 10, no. 5, pp. 612–621, May 2011.

[15] O. Kaltiokallio, H. Yiğitler, and R. Jäntti, "A three-state received signal strength model for device-free localization," *IEEE Transactions on Vehicular Technology*, vol. 66, no. 10, pp. 9226–9240, Oct 2017.

[16] H. Yiğitler, O. Kaltiokallio, and R. Jäntti, "A management framework for device-free localization," in *The 2013 International Joint Conference on Neural Networks*, 2013, pp. 1–8.

[17] M. Bocca, O. Kaltiokallio, and N. Patwari, "Radio tomographic imaging for ambient assisted living," in *Evaluating AAL Systems Through Competitive Benchmarking*, ser. Communications in Computer and Information Science, S. Chessa and S. Knauth, Eds. Springer Berlin Heidelberg, 2013, vol. 362, pp. 108–130.

[18] Y. Bar-Shalom and X.-R. Li, *Estimation with Applications to Tracking and Navigation*. New York, NY, USA: John Wiley & Sons, Inc., 2001.

[19] M. S. Arulampalam, S. Maskell, N. Gordon, and T. Clapp, "A tutorial on particle filters for online nonlinear/non-Gaussian Bayesian tracking," *IEEE Transactions on Signal Processing*, vol. 50, no. 2, pp. 174–188, Feb 2002.